Atmos. Chem. Phys. Discuss., 15, 25231–25267, 2015
www.atmos-chem-phys-discuss.net/15/25231/2015/
doi:10.5194/acpd-15-25231-2015

Atmospheric Chemistry and Physics Discussions

Towards a first classification of aerosol shrinkage events

E. Alonso-Blanco[1], F. J. Gómez-Moreno[1], L. Núñez[1], M. Pujadas[1], M. Cusack[2], and B. Artíñano[1]

[1]Research Center for Energy, Environment and Technology (CIEMAT), Avenida Complutense 40, 28040 Madrid, Spain
[2]Insitute of Chemical Process Fundamentals of the CAS, v.v.i., Rozvojova 135, 165 02, Prague 6, Czech Republic

Received: 6 July 2015 – Accepted: 23 August 2015 – Published: 16 September 2015

Correspondence to: E. Alonso-Blanco (elisabeth.alonso@ciemat.es)

Published by Copernicus Publications on behalf of the European Geosciences Union.

Abstract

This work presents for the first time a classification of shrinkage events based on the aerosol processes that precede them. To this end, 3.5 years of continuous measurements (from 2009 to 2012) of aerosol size distributions, obtained with a Scanning Mobility Particle Sizer (SMPS) at an urban background site in Southern Europe, have been interpreted.

48 shrinkage events were identified and analysed, all occurring during spring and summer when the atmospheric conditions are more favourable for their development. In this study the shrinkage events took place mostly towards the end of the day, and their occurrence could be associated to atmospheric dilution conditions and a reduction in photochemical activity. The shrinkage rate (SR) varied between −1.0 and −11.1 $nm\,h^{-1}$ (average value of $-4.7 \pm 2.6\,nm\,h^{-1}$). Changes in particle concentrations corresponding to the nucleation and Aitken modes were detected, whereby an increase in the number of particles in the nucleation mode often coincided with a reduction in the Aitken mode. The accumulation mode did not undergo significant changes during these processes. In addition, in some cases, a dilution of the total particle number concentration in the ambient air was observed.

Following the proposed methodology, three groups of events have been identified: Group I (NPF + shrinkage), Group II (aerosol growth process + shrinkage) and Group III (pure shrinkage events). The largest number of shrinkage events has been observed in the absence of prior processes, i.e. pure shrinkage events, followed by Group I events and finally Group II events.

Although this analysis has confirmed that the triggering of shrinkage events is clearly linked to the atmospheric situation and the characteristics of the measurement area, this classification may contribute to a better understanding of the processes involved and the features that characterize shrinkage events.

ACPD
15, 25231–25267, 2015

1 Introduction

Particle size is one of the most important properties of atmospheric aerosols (Hinds, 1999; Seinfeld and Pandis, 2006). This property determines the aerosol's physical and chemical characteristics such as its hygroscopicity (Sjogren et al., 2008) or optical properties, and consequently the processes wherein aerosols are involved, such as the ability to form Cloud Condensation Nuclei (CCN) (Dusek et al., 2006; Henning et al., 2002) or the processes of absorption/scattering of solar radiation in the atmosphere (Seinfeld and Pandis, 2006). Thus, aerosol size is a key property in the context of the impact of atmospheric particulates on human health (Englert, 2004), air quality (Charlson, 1969; Quan et al., 2014) and climate change (Lohmann and Feichter, 2005; IPCC, 2013).

Initially, the aerosol size depends on its genesis. However, the transformations that aerosols may undergo during their lifetime in the atmosphere will affect the particle size evolution (Dubovik et al., 2002).

Traditionally, the studies that analyze changes in aerosol size in the atmosphere have focused mainly on the mechanisms that condition and determine their growth. The environmental conditions, such as photochemical activity and relative humidity, which give rise to coagulation and condensation processes are responsible for the increase in the particle size during the course of different scenarios, such as new particle formation (NPF) (Zhang et al., 2012; Zhu et al., 2013; Guo et al., 2012) or combustion processes (Adler et al., 2011; Janhäll et al., 2010; Saarikoski et al., 2007). However, because of the many variables involved in the triggering of particle size reduction under real atmospheric conditions, the number of works which focus on this shrinkage phenomenon is scarce. In fact, the published works on this process are centered mainly on primary emissions of organic particles generated by traffic, due to the high content of semivolatile organic compounds in traffic emissions. These studies are more limited to experimental testing in laboratory settings, or predictive models supplemented by measurements under atmospheric conditions (Robinson et al., 2007; Shrivastava

ACPD
15, 25231–25267, 2015

et al., 2006). Particle size reduction in traffic emissions has also been seen as a consequence of the atmospheric vertical dispersion processes (Dall'Osto et al., 2011).

In this last context, all authors agree on the fact that the processes of dilution, evaporation and chemical aging of semivolatile organics appear to be the mechanisms that contribute to the reduction of the particle size (Donahue et al., 2006; Shrivastava et al., 2006; Robinson et al., 2007; Hitchins et al., 2000). These mechanisms control the partitioning of semivolatile species between the particle phase and gas phase in order to maintain the balance between both phases.

Works found in the literature focusing on particle size reduction in the atmosphere have referred to this process as shrinkage (Young et al., 2013; Cusack et al., 2013; Skrabalova et al., 2015), aerosol growth reversals (Yao et al., 2010; Skrabalova et al., 2015) or shrunken particle size (Yao et al., 2010). All of these terms refer to a progressive reduction of the particle size as a result of the displacement of condensed semivolatile species from the particle phase to the gas phase, due to thermodynamic variations in the ambient conditions for a sufficiently long time that allows for its observation.

These processes have been identified in locations widely-separated geographically and therefore in measurement areas with rather different climates. On the Asian continent, Yao et al. (2010) documented these processes at a coastal suburban site and Young et al. (2013) observed shrinkage processes at a coastal, urban and downwind site. Both authors identified the shrinkage processes in subtropical climates. On the American continent, Backman et al. (2012) detected these processes at an urban background site also in a subtropical climate. In Europe, Cusack et al. (2013) studied these processes at a regional background site with a Mediterranean climate and Skrabalova et al. (2015) identified shrinkage processes at the urban background station in a continental climate. In some of these works, these processes have been identified mainly during NPF, particularly in the growth phase of newly nucleated particles (Yao et al., 2010; Young et al., 2013; Cusack et al., 2013; Skrabalova et al., 2015), but some authors have also documented them in the absence of NPF (Cusack et al., 2013;

ACPD
15, 25231–25267, 2015

Backman et al., 2012). In these studies, all cases were identified during measurement campaigns or periods of continuous measurements ranging from seven to 24 months.

In these articles aerosol growth reversals have been attributed to changes in environmental conditions. The following three factors have been identified as causing these processes:

1. Wind speed: atmospheric dilution caused by an increase in the wind speed triggers changes in the concentrations of the atmospheric gaseous chemical compounds and consequently the partitioning of the semivolatile species from the particle phase to the gas phase in order to maintain the balance between both phases.

2. Air temperature: an increase in the ambient temperature facilitates the evaporation of water and/or condensed semivolatile species which can produce a reduction in the particle size.

3. Photochemical activity: the degree of photochemical oxidation modifies the availability and concentration of chemical species in the atmosphere and, consequently, the distribution of chemical species between particle and gas phases.

This paper proposes the first known classification of shrinkage processes and presents the results obtained for a 3.5 year time-series of measurements at an urban background site located in Madrid (Spain). These phenomena have been classified according to the aerosol processes which preceded the shrinkage event and studied in order to further analyze the possible causes that lead to their development. For each identified event the growth/shrinkage rate has been calculated and an analysis of the evolution of the particle size distribution has been carried out, including the study of the influence of meteorological variables on all these processes.

ACPD
15, 25231–25267, 2015

2 Measurement site

This study has been carried out at an experimental site located in the CIEMAT facilities (40°27′23.2″ N, 03°43′32.3″ E), an urban background area situated approximately 9 km north-northwest of Madrid downtown, and near to three big green areas: Dehesa de la Villa Park, Casa de Campo Park and the Monte del Pardo forest area (Fig. 1). Madrid is located in the center of the Iberian Peninsula, at an average altitude of 650–700 m a.s.l. The city has a high population density, greater than 5000 inhabitants km^{-2}, and is the most populated metropolitan area of Spain, with about 6 million inhabitants. The industrial activity of the region, essentially formed of light industry located mainly in peripheral municipalities of Madrid city, is not significant in terms of atmospheric pollutant emissions. This means that the two main sources of pollution in the city are traffic and heating systems in winter time (Salvador et al., 2012, 2004).

The Madrid region is surrounded by the Sierra de Guadarrama mountain range to the north and by Sierra de Ayllon to the northeast, both belonging to the Central System and situated approximately at a distance of 50–70 km from the metropolitan area. This mountain range (2200 m highest peak) influences the atmospheric dynamics and wind patterns in the study region, especially under specific meteorological conditions.

The normal climatological values recorded in these stations reflect a Continental-Mediterranean climate (Köppen classification) influenced by urban features.

3 Methodology

3.1 Measurements

SMPS measurements in this study were obtained between 2009 and 2012. This instrument consists of a Differential Mobility Analyser (TSI-SMPS: DMA 3081) connected to a Condensation Particle Counter (CPC; TSI Model 3775). The SMPS allows to measure the submicron aerosol fraction into 107 channels (14–700 nm), based on differen-

ACPD
15, 25231–25267, 2015

tial electrical mobility classification, operated in the scanning mode (Wang and Flagan, 1990). Both the equipment control and the data acquisition were conducted using the AIM (Aerosol Instrument Manager) programme developed by TSI Company. The temporal resolution of measurements was 4.5 min.

The equipment was checked and maintenance activities were carried out frequently throughout the whole study period. Furthermore, the response of the equipment was verified during the intercomparison campaigns of the Spanish Network on Environmental DMAs (REDMAAS, in its Spanish acronym) that took place from 2010 to 2012 (Gómez-Moreno et al., 2010, 2015).

The total number of particles (N_t) and particle concentrations for each of the three modes: nucleation ($N_{<30\,nm}$), Aitken ($N_{30–100\,nm}$) and accumulation ($N_{>100\,nm}$), were obtained from the aerosol size distributions. The choice of the intervals of particle sizes that define each of the modes is based on the classification developed by Charron and Harrison (2003), while taking into account the measurement size range of the SMPS used in this study.

The monthly data coverage obtained for the 3.5 years of the study is shown in Fig. 2. 69 % of data was available for the entire period with the following distribution of intra-annual data: 70 % in 2009, 56 % in 2010, 70 % in 2011 and 80 % in 2012.

Data loss during the measurement period was due to regular calibration, normal maintenance activities, equipment breakdown or transfer of the equipment to another measurement site. It is necessary to point out that, from June to December 2012, technical problems in the first nine channels of the SMPS were detected, and therefore those data have not been taken into account in the data processing.

A permanent meteorological station 52 m high installed in the CIEMAT facilities provided meteorological records of precipitation, pressure, irradiance, temperature, relative humidity (RH), precipitation, wind speed and wind direction. The meteorological sensors of this station are calibrated twice a year, in the winter and summer periods. These data are averaged and recorded automatically every 10 min.

ACPD
15, 25231–25267, 2015

To characterize the air mass composition arriving at the sampling point, a Differential Optical Absorption Spectrometer (DOAS) provided data of gaseous pollutants, such as NO, NO_2 and O_3 (Platt and Stutz, 2008). This DOAS system (OPSIS AR-500) operated with an optical path of 228 m at an average height of 10 m a.g.l. The temporal resolution of the equipment for all of the species measured was about 7 min. The DOAS calibration routine is performed once a year based on calibration cells and reference gases.

Furthermore, standard information on air quality in the measurement area was provided by the suburban station of Casa de Campo (3°44′50.44″ W, 40°25′09.68″ N, 645 m a.s.l. and 4.5 km southwest from the experimental site). This station is one of the 24 automatic stations belonging to the Air Quality Monitoring Network of the Madrid municipality. SO_2, NO_x and O_3 hourly average concentrations measured in Casa de Campo station complemented the DOAS data obtained in CIEMAT.

3.2 Methodology applied for studying shrinkage events

3.2.1 Identification of shrinkage events

The methodology proposed by Dal Maso et al. (2005) to identify NPF and subsequently described in detail by Kulmala et al. (2012) has been adapted in this work to identify and study the shrinkage processes.

This methodology allows for the observation of the evolution of aerosol size distributions in the atmosphere by surface plots representing the particle size distributions as a function of time. These types of graphs were made on a daily basis (24 h), from 00:00 UTC on the first day to 00:00 UTC on the next day for the whole measurement period.

Given the data coverage of all the measurements that were collected, thus giving an extensive and representative database, a classification of shrinkages could be carried out. Based on a visual analysis of the daily surface plots, the aerosol growth reversals have been categorized into three groups according to the processes that precede them:

ACPD
15, 25231–25267, 2015

1. Group I, NPF + shrinkage events: shrinkages produced during the growth phase of the newly nucleated particles. In turn, NPF type has been identified according to the methodology developed by Dal Maso et al. (2005) in Ia and Ib.

2. Group II, aerosol growth process + shrinkage events: shrinkages which occurred during the process of growth of atmospheric aerosol, with no previous NPF.

3. Group III, pure shrinkage events: shrinkages that took place in the absence of a specific previous process.

In this paper, the authors have considered an event as the sum of the process that precedes the shrinkage (NPF or aerosol growth process) and the shrinkage process itself.

In the identification of these events, the evolution of the aerosol size distribution and the meteorological and air mass changes have been taken into account in order to identify mixtures of air masses, which may be responsible for "apparent shrinkages". Most of the identified events showed a uni-modal size distribution.

Changes in aerosol concentrations due to dilution processes have also been studied. In this paper, the authors have considered the presence of dilution when the ratio between the two event phases (NPF or aerosol growth process phase vs. shrinkage phase) was higher than 10 %, coinciding with the measurement uncertainty established in the ACTRIS SMPS standards (Wiedensohler et al., 2010).

Additionally, the growth rate (GR) during these events was calculated as outlined by Kulmala et al. (2012). The particle shrinkage rate (SR) was estimated using the same equation as for GR, with the resulting value being negative. The calculation was made from the mode/s of the aerosol size distributions averaged every 15 min (D_{mode}). The aerosol size distributions were fitted to a lognormal function to estimate the modes.

Finally, the calculation of the condensation sink (CS) and an estimation of H_2SO_4 concentration in gas phase have been incorporated in this work for the shrinkage study of Group I (NPF + shrinkage events).

ACPD
15, 25231–25267, 2015

Calculation of the condensation sink

The aerosol condensation sink (CS) determines how rapidly molecules will condense onto pre-existing aerosols and depends strongly on the shape of the size distribution (Pirjola et al., 1999; Lehtinen et al., 2003). NPF takes place during periods in which the CS is low because it indicates that the concentration of condensable gases present in the atmospheric is high.

The CS has been calculated according to Kulmala et al. (2001) and is defined by the expression (1):

$$\mathrm{CS} = 2\pi D \sum_{i}^{0} \beta_{M\cdot i} d_{\mathrm{p}i} N_i \quad (1)$$

Where: D is the diffusion coefficient ($\mathrm{cm^2\,s^{-1}}$); $\beta_{M\cdot i}$ is the transitional correction factor, $d_{\mathrm{p}i}$ (nm) is the particle diameter and N_i ($\mathrm{cm^{-3}}$) is the particle number concentration for each particle size discrete interval i.

Estimation of H_2SO_4 concentration in gas phase

Sulfuric acid is formed from SO_2 produced, in the case of this study area, mainly by the combustion of fossil fuels in motor vehicles and heating devices. A complete description of the chemical reactions that lead to the formation of H_2SO_4 can be found in Seinfeld and Pandis (2006).

Many authors suggest that gas-phase sulphuric acid is the main initiating agent of nucleation processes (Fiedler et al., 2005; Kusaka et al., 1998; Kulmala and Laaksonen, 1990; Kulmala et al., 2000), which makes its study of utmost importance during NPF.

In this work, sulfuric acid in the gas phase [H_2SO_4] has been estimated following the mathematical model developed by Mikkonen et al. (2011), which is expressed by

ACPD
15, 25231–25267, 2015

Eq. (2):

$$[H_2SO_4] = 8.21 \times 10^{-13}\ \kappa\ \text{Radiation}\ [SO_2]^{0.62}\ (\text{CS}\ \ \text{RH})^{-0.13} \quad (2)$$

Where: κ is the reaction rate constant, which is calculated according to Eq. (3) in Mikkonen et al. (2011), and is scaled by multiplying it with 10^{12} ($m^2\,W^{-1}\,s^{-1}$); Radiation is global radiation ($W\,m^{-2}$), [SO_2] is the measured SO_2 concentrations ($molec\,cm^{-3}$); CS is the condensation sink (s^{-1}); and RH is the relative humidity (%).

The estimation of H_2SO_4 in gas phase using this model is highly dependent on solar radiation because the availability of certain chemical compounds involved in their formation have a strong dependence on photochemical activity (Stanier et al., 2004; Mikkonen et al., 2011). This implies that the concentration of H_2SO_4 exhibits the same diurnal pattern as the solar radiation.

4 Results and discussions

4.1 Time series analysis

A total of 48 shrinkage events were observed during the study period. The number of cases identified was irregularly distributed over the four years. In 2010 and 2012, the number of shrinkages identified was 21 and 16 respectively, whereas only seven and four cases were observed in 2009 and 2011 respectively (Fig. 3). The difference in the number of cases identified between both groups of years did not seem to be motivated by bias of the database as a consequence of the data loss. The study of the evolution of the monthly and daily averages of the meteorological parameters recorded during the four years of study showed no significant interannual variations, nor for the annual averages (temperature of $15.2 \pm 0.5\,^{\circ}C$; wind speed of $3.4 \pm 0.2\,m\,s^{-1}$, RH of $56 \pm 5\,\%$ and irradiance of $180 \pm 5\,W\,m^{-2}$). This is consistent with data provided by the Spanish National Agency for Meteorology (AEMET) for the Madrid regional stations. Therefore,

ACPD
15, 25231–25267, 2015

meteorological factors can be discarded as the cause of this observed difference in the inter-annual occurrence of shrinkage events.

The occurrence of shrinkage has been detected only during spring and summer seasons, in the months of May, June, July and August, when the necessary conditions occur. On the one hand, the higher solar irradiance during spring and summer enhances photochemical activity. On the other hand, higher photosynthetic activity results in higher emissions of biogenic volatile organic compounds (BVOCs) from vegetation. Thus, during these periods there was increased production and availability of gaseous chemical compounds (precursors) in the atmosphere which facilitate NPF and also the growth of preexisting particles. This process has been described previously in some studies (Dal Maso et al., 2009; Eerdekens et al., 2009). Moreover, the atmospheric dynamics in the study area during these months, mostly local air flows and recirculation processes, gave rise to an increased residence time of aerosols in the atmosphere, therefore making the aerosols prone to suffer more changes during their prolonged atmospheric lifetime. This was evidenced by the significant number of NPF and growth processes observed during the period studied, which often took place on the same days as the shrinkage events.

The greater number of shrinkages observed in June and July compared to May and August (Fig. 3) was probably due to the predominance of the optimal environmental conditions during June and July (average meteorological values for June and July compared to May and August during the 3.5 years of study: temperature 24.4 ± 0.7 vs. $22.2 \pm 0.8\,^{\circ}\mathrm{C}$; wind speed 3.7 ± 0.3 vs. $3.5 \pm 0.1\,\mathrm{m\,s^{-1}}$; RH 37 ± 6 vs. $42 \pm 5\,\%$ and irradiance 292.9 ± 12.7 vs. $260.2 \pm 7.7\,\mathrm{W\,m^{-2}}$). The scarce number of events identified in July 2011 (only two case studies) was attributed to the lack of data coverage.

The highest number of cases observed corresponded to pure shrinkage events whereas the less frequent were those of aerosol growth process + shrinkage events.

A summary of the five shrinkage studies found in the literature, and the present work, is given in Table 1. All shrinkages have been identified under temperate climates, with the exception of Skrabalova et al. (2015). The climatic characteristics of each

ACPD
15, 25231–25267, 2015

region determined the temporal variability observed in these processes. However, the occurrence of particle shrinkage was mainly observed on the warm seasons.

Except for those of Cusack et al. (2013), all cases have occurred in measurement areas with a clear influence of anthropogenic emissions. Furthermore, the shrinkage events took place in the middle of the day (around 12:00 UTC) (Fig. 4a), contrasting with the cases identified in this study where the shrinkage phases were triggered around 18:00 UTC (Fig. 4b).

The studies related to aerosol shrinkages concluded that atmospheric dilution and the high ambient temperature were found to be the main causes of all these processes (Table 1), and exceptionally a decrease in photochemical activity as Yao et al. (2010) and Skrabalova et al. (2015) pointed out in their papers.

In the present work, the atmospheric dilution was the leading cause of the reduction in particle size, the 80 % of the shrinkage processes occurred under a wind speed that exceeded 4 $m\,s^{-1}$. However, shrinkages were also identified as a result of the reduction of the photochemical activity that occurred at the end of day, especially in the NPF + shrinkage events. Temperature did not appear to be a decisive feature in the development of these processes.

As a consequence of the particle size reduction, a displacement of particle concentrations towards smaller size modes was observed. Furthermore, in some case studies, the shrinkage was accompanied by a reduction in the concentration of total number of particles, which exceeded 25 % for some events.

In the following sections, the formation patterns of each type of shrinkage event outlined previously will be discussed based on a selected case study chosen as an example.

ACPD
15, 25231–25267, 2015

4.2 Case study analysis

4.2.1 Group I: NPF + shrinkage events

Shrinkage processes were identified during the growth phase of the newly nucleated particles in 17 cases. The shrinkages were mainly observed during NPF of type Ia, and a minority in NPF of type Ib, with 13 and 4 cases, respectively. The duration of these events ranged between 7 and 14.75 h including the new particle formation, growth and subsequent growth reversals. The shrinkage phase lasted less than the NPF phase, between 0.75 and 5 h. Exceptionally, three NPF + shrinkage events in which several processes of growth and shrinkage occurred were also identified.

These types of events typically started between 09:00 and 12:00 UTC (Fig. 4a), when the conditions were suitable for NPF development i.e. low concentrations of preexisting particles in the atmosphere (low CS); high solar activity; and low relative humidity (Hamed et al., 2011). In addition, NPF was typically observed in the measurement area when the CIEMAT site was downwind of big green areas, that is, under wind directions from W to N sector (El Pardo forest area) and from S to W sector (Casa de Campo Park). This effect has been already observed in the measurement area and described by Gómez-Moreno et al. (2011). The origin of these air masses suggests the presence of high concentrations of BVOCs, which favor the growth of the newly nucleated particles.

At the beginning of the NPF phase, the average D_{mode} was 22.5 ± 5.3 nm, increasing to 43.8 ± 11.2 nm by the end of the growth phase. The observed GR ranged from 1.5 to 10.6 nm h^{-1}. In some of these case studies, D_{mode} could not be estimated at the start of NPF because it was below the detection limit of the instrument. During the shrinkage phase, the average D_{mode} decreased from 43.8±11.2 to 33.2±9.2 nm with a SR ranging from −1.5 to −10.2 nm h^{-1}. The SR estimated in the present study is within the range of those reported in the aerosol shrinkage studies listed in Table 1. However, given

ACPD
15, 25231–25267, 2015

the high diversity of possible scenarios under which shrinkage may occur, valid direct comparisons between any given case are somewhat difficult.

During these events, the wind circulation in the study area played an important role. During the months that shrinkages were identified, as a result of the high solar radiation, local air flows were thermally driven and the wind direction in the area followed a well-defined pattern (Salvador, 2004; Artíñano et al., 1994; Plaza and Artíñano, 1994; Artíñano et al., 2003; Pujadas et al., 2000). At night (21:00–08:00 UTC) flows had a dominant NE–ENE origin, whereas during the daytime (09:00–20:00 UTC) the dominant origin sector was SW–WSW. The wind direction after noon maintained a directional component from the SW, when the daily wind speed reached the maximum value. In these cases, an early and atypical change of the wind direction towards the NE sector that occurred around 18:00 UTC, accompanied by an increase in wind speed, was responsible for a significant number of shrinkages. The factors that determine this change in the wind pattern could not be identified, and could probably attributed to a transition regime associated to a change of the pressure field at synoptice scale.

Case study: 1 July 2012

An example of a shrinkage process associated with NPF of type Ia was observed on 1 July 2012 (Fig. 5). This event lasted 8.5 h; 4.5 h corresponding to the nucleation phase and 4 h to the shrinkage phase.

The event took place under clean air mass conditions, as demonstrated by the low and invariable concentrations of pollutant gases NO and NO_2. The diurnal variation of O_3 concentrations indicates significant photochemical activity.

NPF phase began at 11:15 UTC and concluded at 15:45 UTC. The wind speed and direction remained constant throughout the NPF event. The average wind speed was low ($2.8 \pm 1.1\,m\,s^{-1}$), indicating limited atmospheric horizontal dilution, and the prevailing wind direction came from sector W–N. As indicated previously, the air masses that arrived at the measurement site under these wind directions possibly transported

ACPD
15, 25231–25267, 2015

BVOCs from the nearby green areas, thus facilitating NPF and growth of the freshly formed particles.

As shown in Fig. 5, high solar radiation (943 $W\,m^{-2}$ at 13:00 UTC), coupled with sufficient gas phase sulfuric acid (4.0×10^7 molec cm^{-3}) and a probable source of BVOCs provided suitable conditions for NPF to occur. In addition, a low background concentration of pre-existing particles was recorded when nucleation commenced, as highlighted by the low CS (from $4.9 \times 10^{-3}\,s^{-1}$ at 11:15 UTC to $7.6 \times 10^{-3}\,s^{-1}$ at 15:45 UTC). The CS behavior observed in this work is in accordance with that described in other studies focused on NPF (Cusack et al., 2013; Yao et al., 2010; Young et al., 2013; Vehkamäki et al., 2004). During the NPF, the GR was 7.2 $nm\,h^{-1}$. D_{mode} increased from 21.1 nm at 12:00 UTC to 46.8 nm at 15:45 UTC.

Furthermore, the evolution of the concentration of particles corresponding to each of the three modes was characteristic of this type of process (Guo et al., 2012; Du et al., 2012; Shen et al., 2011). From 11:15 until 13:15 UTC, the nucleation mode was the main contributor to the total particle concentration (above 50 %), while after 13:15 UTC and due to growth of freshly nucleated particles, the main contributor to the total concentration was the Aitken mode, with more than 50 % of the total. This trend continued until the end of the NPF event.

The beginning of the shrinkage phase occurred at 15:45 UTC, when D_{mode} was 46.8 nm, reducing to 31.5 nm by the end of the event. This coincided with a wind speed increase, from $2.8 \pm 1.1\,m\,s^{-1}$ during NPF to $4.6 \pm 1.0\,m\,s^{-1}$ during the shrinkage, but with no considerable change in wind direction. At 18:20 UTC, the wind direction shifted to the N–E sector, and remained unchanged until the end of the shrinkage event, at 19:45 UTC. The shrinkage event also appears to coincide with the reducing solar radiation as the day continues. The reduction in irradiance would lead to a reduction in the photochemical production of condensable semivolatile vapours. This, combined with atmospheric dilution as a result of the increased wind speed, may have resulted in a change in the equilibrium of gas/particle portioning, allowing for the shrinkage process to occur. However, the noticeable increase in the wind speed that triggered

ACPD
15, 25231–25267, 2015

the development of the shrinkage did not lead to dilution of the ambient particulate concentration as would be expected. The average particle concentration during NPF was $7 \times 10^3 \pm 2 \times 10^3$ particles cm^{-3}, while concentrations during the shrinkage were $8 \times 10^3 \pm 0.4 \times 10^3$ particles cm^{-3}. As particles shrunk in size, they transitioned from the Aitken mode to the nucleation mode. By the end of the shrinkage event, the nucleation mode contributed 44 % to the total particle number concentration. This variation in particle concentrations corresponding to both modes during the shrinkage events has been reported previously (Young et al., 2013; Cusack et al., 2013). The accumulation mode did not show a significant change during this phase, contributing 5 % to the total particle concentration. The SR for this shrinkage event was -3.8 nm h^{-1}.

4.2.2 Group II: aerosol growth process + shrinkage events

A type of shrinkage process not previously documented in the literature is the shrinkage associated with a previous aerosol growth event in the absence of nucleation.

Nine aerosol growth process + shrinkage (Group II) events have been identified during the period of this study. These events lasted between 2.0 and 13.5 h. Depending on the time of day at which these events were identified, and consequently determining the mechanisms of the particle growth, two subgroups of Group II events have been differentiated.

Three events corresponded to the first subgroup (Group IIa). The growth phase occurred at noon, between 12:00 and 14:00 UTC (Fig. 4), under stagnant conditions (wind speed around 2 m s^{-1}). These cases were characterized by a high ambient particle concentrations during the early morning hours, between 07:00 and 09:00 UTC, as a result of traffic emissions typical of the study area (Gómez-Moreno et al., 2011). Under these conditions, the aerosols grew in the absence of dilution which was enhanced by high photochemical activity and also the arrival of air masses from the El Pardo forest area (NW sector) and Casa de Campo Park (SW sector), providing BVOCs that facilitated the particle growth.

ACPD
15, 25231–25267, 2015

The growth phase of these events lasted between 4.5 and 6.5 h. During this phase, D_{mode} went from 40.5 ± 15.7 to 63.4 ± 21.9 nm and their GR varied between 2.8 and 5.6 nm h^{-1}. The duration of the shrinkage phase ranged between 1.5 and 7 h, with D_{mode} decreasing to an average diameter of 52.5 ± 25.8 nm with a SR between −2.3 and −3.3 nm h^{-1}.

Six events fit in the second subgroup (Group IIb). These events occurred during the late afternoon, around 18:00 UTC (Fig. 4), and were produced under polluted air masses with traffic emissions. An increase in concentrations of NO and NO_2 was observed during these events. The growth and shrinkage phases occurred during a period with high wind speeds, 5.6±1.2 and 5.2±1.7 m s^{-1} respectively, and a constant wind direction. These particles initially experienced significant growth, D_{mode} from 50.8 ± 13.3 to 56.2 ± 14.0 nm, with a GR ranging between 3.6 to 9.4 nm h^{-1}, for a brief period no longer than 2 h. Later on, the aerosol suffered a gradual decrease in the particle size, from 56.2±14.0 to 44.0±10.1 nm, with a SR which varied between-3.2 and −6.9 nm h^{-1}. This phase was longer than the growth phase, lasting between 1.3 and 4.3 h.

Aerosol growth process + shrinkage events possibly happened mainly due to the loss in the content of volatile organic compounds (VOCs) from aerosol emitted by traffic under high dilution conditions.

Case study: 31 May 2010–1 June 2010

A clear example of this group was the shrinkage event observed on 31 May and 1 June 2010 (Fig. 6).

This event commenced at 13:00 UTC on 31 May and continued until 02:30 UTC on 1 June, lasting 13.5 h; 6.5 h corresponding to the growth phase and 7 h to the shrinkage phase.

On 31 May, significant traffic emissions affected the measurement site between 05:30 and 07:00 UTC. The average particle concentration was $25 \times 10^3 \pm 7 \times 10^3$ particles cm^{-3}. The average wind speed from 00:00 to 18:00 UTC was very light

ACPD
15, 25231–25267, 2015

($2.2 \pm 0.9\,m\,s^{-1}$), indicating limited aerosol dispersion and reduced horizontal mixing and dilution. NO_2 concentrations, measured at the Casa de Campo station, were also elevated, with a mean value of $26.4 \pm 13.8\,\mu g\,m^{-3}$, verifying the polluted state of the air mass.

Under this situation, the growth phase emerged at 13:00 UTC and ended at 19:30 UTC. D_{mode} increased from 36.2 to 55.0 nm, with a GR of $2.8\,nm\,h^{-1}$. During this period, the average irradiance and temperature were $486 \pm 334\,W\,m^{-2}$ and $32.3 \pm 1.3\,^{\circ}C$ respectively, and the average wind speed was $2.7 \pm 1.5\,m\,s^{-1}$, with a dominant directional component around WSW and W (Casa de Campo Park). As suggested previously, high photochemical production of semi-volatiles and high vegetative emissions would likely have provided suitable conditions for aerosol growth.

Between 19:30 and 02:30 UTC the shrinkage phase emerged. D_{mode} decreased from 55.0 to 32.0 nm, with a SR estimated of $-3.3\,nm\,h^{-1}$. At 19:30 UTC, there was a change in the wind direction from the component WSW–W to NE accompanied by an increase in wind speed. This situation remained until 02:30 UTC. The wind speed was $4.8 \pm 0.8\,m\,s^{-1}$, double the wind speed registered during the aerosol growth phase. Moreover, the absence of photochemical activity during this second phase inhibited the formation of secondary chemical compounds in the atmosphere. Thus, the dilution of the gaseous components in the atmosphere, together with the reduction in the formation of new chemical compounds by photochemical processes, were the likely causes for initiating the observed shrinkage, as seen in the previous case study.

During the aerosol growth phase, the Aitken mode is the dominant mode, followed by the nucleation and accumulation modes. However, as in the NPF + shrinkage (Group I) events, concentrations of nucleation mode particles grew at the expense of the Aitken mode. At the beginning of the shrinkage event, the nucleation mode contributed 15 % of the total particle concentration, vs. 80 % of the Aitken mode. At the end of the event, the contributions of both modes were 45 and 47 %, respectively.

The wind speed increase was associated not only with a significant reduction in the particle size but also in a reduction in the particle number concentration. A 24 %

ACPD
15, 25231–25267, 2015

decrease of the total particle concentration was observed during the shrinkage phase. During this phase, N_t was $10 \times 10^3 \pm 0.8 \times 10^3$ vs. $13 \times 10^3 \pm 1.7 \times 10^3$ particles cm^{-3} measured during the aerosol growth phase. This reduction corresponded to decreases in the Aitken and accumulation mode particle concentrations, with a contribution of 28 and 51 % respectively.

4.2.3 Group III: pure shrinkage events

Shrinkage processes have also been observed in the absence of a preceding NPF event or particle growth process. Twenty two pure shrinkage events were identified during the 3.5 years of this study. Two cases were observed on the same day coinciding with the arrival of two different types of air masses to the measurement area.

Most of these cases were identified during a period of high wind speeds, normally higher than the previous two hours i.e. average wind speeds of 6.0 ± 1.8 vs. 4.3 ± 2.2 m s^{-1}. Furthermore, these events have been observed under different wind directions; around WNW and SW sectors (El Pardo forest area and Casa de Campo Park) and around the NE sector. Pure shrinkage events were noticed both under clean conditions, associated to the biogenic secondary organic aerosol transport from the vegetated areas close to the CIEMAT, in the first case, and under polluted conditions, when the NO and NO_2 concentrations suffered a significant increase relative to the previous two hours, indicating a clear traffic origin, in the second case.

The shrinkage in this group had a longer duration compared with the shrinkage phases of the other types of events analyzed, with an average of 4 h (between 1.75 and 8.5 h). On average, the particle size decreased from 55.9 ± 16.2 to 39.3 ± 12.2 nm giving rise to variations of SR from -1.0 to -11.1 nm h^{-1}.

As it was similarly hypothesized for the Group II: aerosol growth process + shrinkage events, the pure shrinkage events were principally a result of the loss of volatile and semi-volatile organic vapours from biogenic aerosols or emitted by traffic under suitable dilution conditions.

ACPD
15, 25231–25267, 2015

Case study: 29 July 2010

An example of a pure shrinkage event was identified on 29 July 2010 (Fig. 7), which lasted 4 h.

The aerosol growth reversal occurred under cleaned air masses which transported a significant concentration of biogenic secondary organic aerosol. The cleaned air plumes began to arrive at the study site from the green areas near the CIEMAT at 14:00 UTC, when the wind direction changed from a fluctuating direction to a clear dominance of the W–N sector. This change was also accompanied by an increase in the wind speed, from < 3 to $> 5\,m\,s^{-1}$ after 14:00 UTC.

The NO_2 concentration suffered a slight increase from 14:00 UTC until 00:00 UTC on 30 July 2010, during which time the average concentrations were $11.8 \pm 4.5\,\mu g\,m^{-3}$, while the NO concentration did not undergo significant change.

The shrinkage began at 16:15 UTC and ended at 20:15 UTC, during which the D_{mode} changed from 55.0 to 27.5 nm, and the SR was $-7.3\,nm\,h^{-1}$. The average particle concentration during the shrinkage event was $13 \times 10^3 \pm 1.9 \times 10^3$ particles cm^{-3}, reaching the maximum concentration around 19:30 UTC, when concentrations of 16×10^3 particles cm^{-3} were exceeded. After that moment a gradual reduction in the particle concentration was observed, giving concentrations of 12×10^3 particles cm^{-3} by the end of the event.

As occurred in the rest of the events, changes in concentrations corresponding to each mode were also observed. Between 16:15 and 18:00 UTC, the Aitken mode was the main contributor to the total particle concentration, accounting for over 80 % of the total particles measured. From 18:00 until 20:15 UTC, when the shrinkage ended, a gradual increase in the nucleation mode occurred simultaneously with a gradual decrease in the Aitken mode. At the end of the event, the nucleation mode was the main contributor (59 %) to the concentration of total particles. The accumulation mode did not undergo significant variations and the ambient particle number concentration re-

ACPD
15, 25231–25267, 2015

mained elevated throughout the event, indicating there was no significant dilution of the submicrometer atmospheric aerosol measured.

In this case study, the particle size reduction, and consequently the variations in the particle concentrations corresponding to each mode, seemed to be a result of the loss of BVOCs from biogenic aerosol during a period of high atmospheric dilution. In addition, the decrease in irradiance would produce a decrease in the photochemical activity, and therefore, a reduction in the photochemical formation of semivolatile gases.

This type of shrinkage have also been observed by Cusack et al. (2013) and Backman et al. (2012). However, while both authors related these processes to the evaporation of semi-volatile gases from the surface of particles during the hours of maximum solar radiation, in this work they have been identified at the end of the day, mainly as a result of atmospheric dilution caused by a significant increase of wind speed.

5 Conclusions

This paper provides the first study of aerosol shrinkage processes based on a long time series of data covering 3.5 years of measurements. An analysis of this time series has allowed for characterizing the main features of these processes based on 48 cases identified.

All shrinkages occurred during the months of May, June, July and August, when the atmospheric dynamics allowed the aerosol to have a longer residence time in the atmosphere and therefore an extended exposure time to incur physical and chemical changes. In addition, the environmental conditions, mainly intense photochemical activity in the presence of elevated concentrations of BVOCs, facilitated new particle formation and subsequent growth of atmospheric particles.

The shrinkage events identified in this study all occurred during the final part of the day, and were caused mostly by atmospheric dilution by increased wind speeds, 80 % of the shrinkage processes occurred under a wind speed that exceeded 4 $m\,s^{-1}$, and, to a lesser extent, by reductions in photochemical activity.

ACPD
15, 25231–25267, 2015

The shrinkage phases usually had a shorter duration than NPF and aerosol growth phases. The SR values ranged between −1.0 and −11.1 nm h^{-1} (with an average value of -4.7 ± 2.6 nm h^{-1}) for these events.

As a result of the shrinkage, changes in the total particle number concentration and predominantly in the nucleation and Aitken modes were observed. Generally, an increase of particle concentration in the nucleation mode coincided with a reduction in the Aitken mode as particles reduced in size. During some events these changes were not so evident because the particle size reduction was maintained within the Aitken mode. Furthermore, the shrinkages were in some cases accompanied by a reduction in the aerosol concentration.

Based on the identified cases, three types of shrinkage events were proposed: shrinkages proceeded by a new particle formation and growth process (Group I: NPF + shrinkage events), shrinkages proceeded by a growth process in the absence of NPF (Group II: aerosol growth process + shrinkage events) and shrinkages in the absence of any previous process (Group III: pure shrinkage events).

Pure shrinkage events were the most frequent group followed by NPF + shrinkage events, being the least frequent group that of aerosol growth process + shrinkage events.

This work demonstrates that the proposed methodology is suitable for accurately and reliably classifying these processes. In addition, as it has been evidenced in this paper, environmental conditions and typical characteristics of the measurement area (climate, atmospheric dynamics, land use...) are crucial for their development. However, it is necessary to further deepen our understanding of these processes and their dynamics and patterns.

Acknowledgements. This work has been supported by the Spanish National Research Plan through funding of the projects, PHAESIAN (CGL2010-1777), REDMAAS (CGL2011-15008-E), MICROSOL (CGL2011-27020), PROACLIM (CGL2014-52877-R) and by the Madrid Regional Research Plan through TECNAIRE (P2013/MAE-2972). E. Alonso-Blanco acknowledges the FPI grant to carry out the doctoral thesis/PhD at the Research Center for Energy, Environment and Technology (CIEMAT). Thank are also given to José Luis Mosquera for his help in the

ACPD
15, 25231–25267, 2015

processing of data which are the core of this work and Iván Alonso for his help in preparing some of the figures included in this paper.

References

Adler, G., Flores, J. M., Abo Riziq, A., Borrmann, S., and Rudich, Y.: Chemical, physical, and optical evolution of biomass burning aerosols: a case study, Atmos. Chem. Phys., 11, 1491–1503, doi:10.5194/acp-11-1491-2011, 2011.

Artíñano, B., Pujadas, M., Plaza, J., Crespí, S. N., Cabal, H., Aceña, B., and Terés, J.: Air pollution episodes in the Madrid airshed, in: Transport and Transformation of Pollutants in the Troposphere, SPB Academic Publishing, Copenhagen, Denmark, 294–297, 1994.

Artíñano, B., Salvador, P., Alonso, D. G., Querol, X., and Alastuey, A.: Anthropogenic and natural influence on the PM_{10} and $PM_{2.5}$ aerosol in Madrid (Spain). Analysis of high concentration episodes, Environ. Pollut., 125, 453–465, 2003.

Backman, J., Rizzo, L. V., Hakala, J., Nieminen, T., Manninen, H. E., Morais, F., Aalto, P. P., Siivola, E., Carbone, S., Hillamo, R., Artaxo, P., Virkkula, A., Petäjä, T., and Kulmala, M.: On the diurnal cycle of urban aerosols, black carbon and the occurrence of new particle formation events in springtime São Paulo, Brazil, Atmos. Chem. Phys., 12, 11733–11751, doi:10.5194/acp-12-11733-2012, 2012.

Cusack, M., Alastuey, A., and Querol, X.: Case studies of new particle formation and evaporation processes in the western Mediterranean regional background, Atmos. Environ., 81, 651–659, 2013.

Charlson, R. J.: Atmospheric visibility related to aerosol mass concentration: review, Environ. Sci. Technol., 3, 913–918, 1969.

Charron, A. and Harrison, R. M.: Primary particle formation from vehicle emissions during exhaust dilution in the roadside atmosphere, Atmos. Environ., 37, 4109–4119, 2003.

Dal Maso, M., Kulmala, M., Riipinen, I., Wagner, R., Hussein, T., Aalto, P. P., and Lehtinen, K. E. J.: Formation and growth of fresh atmospheric aerosols: eight years of aerosol size distribution data from SMEAR II, Hyytiala, Finland, Boreal Environ. Res., 10, 323–336, 2005.

Dal Maso, M., Hari, P., and Kulmala, M.: Spring recovery of photosynthesis and atmospheric particle formation, Boreal Environ. Res., 14, 711–721, 2009.

ACPD
15, 25231–25267, 2015

Dall'Osto, M., Thorpe, A., Beddows, D. C. S., Harrison, R. M., Barlow, J. F., Dunbar, T., Williams, P. I., and Coe, H.: Remarkable dynamics of nanoparticles in the urban atmosphere, Atmos. Chem. Phys., 11, 6623–6637, doi:10.5194/acp-11-6623-2011, 2011.

Donahue, N. M., Robinson, A. L., Stanier, C. O., and Pandis, S. N.: Coupled partitioning, dilution, and chemical aging of semivolatile organics, Environ. Sci. Technol., 40, 2635–2643, 2006.

Du, J., Cheng, T., Zhang, M., Chen, J., He, Q., Wang, X., Zhang, R., Tao, J., Huang, G., and Li, X.: Aerosol size spectra and particle formation events at urban Shanghai in Eastern China, Aerosol Air Qual. Res., 12, 1362–1372, 2012.

Dubovik, O., Holben, B., Eck, T. F., Smirnov, A., Kaufman, Y. J., King, M. D., Didier, T., and Slutsker, I.: Variability of absorption and optical properties of key aerosol types observed in worldwide locations, J. Atmos. Sci., 59, 590–608, 2002.

Dusek, U., Frank, G. P., Hildebrandt, L., Curtius, J., Schneider, J., Walter, S., Chand, D., Drewnick, F., Hings, S., and Jung, D.: Size matters more than chemistry for cloud-nucleating ability of aerosol particles, Science, 312, 1375–1378, 2006.

Eerdekens, G., Yassaa, N., Sinha, V., Aalto, P. P., Aufmhoff, H., Arnold, F., Fiedler, V., Kulmala, M., and Williams, J.: VOC measurements within a boreal forest during spring 2005: on the occurrence of elevated monoterpene concentrations during night time intense particle concentration events, Atmos. Chem. Phys., 9, 8331–8350, doi:10.5194/acp-9-8331-2009, 2009.

Englert, N.: Fine particles and human health: a review of epidemiological studies, Toxicol. Lett., 149, 235–242, 2004.

Fiedler, V., Dal Maso, M., Boy, M., Aufmhoff, H., Hoffmann, J., Schuck, T., Birmili, W., Hanke, M., Uecker, J., Arnold, F., and Kulmala, M.: The contribution of sulphuric acid to atmospheric particle formation and growth: a comparison between boundary layers in Northern and Central Europe, Atmos. Chem. Phys., 5, 1773–1785, doi:10.5194/acp-5-1773-2005, 2005.

Gómez-Moreno, F., Alonso-Blanco, E., Artíñano, B., Juncal-Bello, V., Iglesias-Samitier, S., Piñeiro Iglesias, M., López Mahía, P., Perez, N., Pey, J., Ripoll, A., Alastuey, A., de la Morena, B., García, M., Rodríguez, S., Sorribas, M., Titos, G., Lyamani, H., Lucas, A.-A., Latorre, E., Tritscher, T., and Bischof, O.: Intercomparisons of mobility size spectrometers and condensation particle counters in the frame of the Spanish atmospheric observational aerosol network, Aerosol Sci. Tech., 49, 777–785, doi:10.1080/02786826.2015.1074656, 2015.

ACPD
15, 25231–25267, 2015

Gómez-Moreno, F. J., Artíñano, B., Piñeiro Iglesias, M., López Mahía, P., Pey, J., Alastuey, A., Sorribas, M., de la Morena, B. A., and Rodríguez, S.: The Spanish network on environmental DMAs: introduction and main activities, IV Spanish Meeting on Aerosol Science and Technology – RECTA 2010, 28–30 June, Granada, Spain, ISBN: 978-84-693-4839-0, 2010.

Gómez-Moreno, F. J., Pujadas, M., Plaza, J., Rodríguez-Maroto, J. J., Martínez-Lozano, P., and Artiñano, B.: Influence of seasonal factors on the atmospheric particle number concentration and size distribution in Madrid, Atmos. Environ., 45, 3169–3180, 2011.

Guo, H., Wang, D. W., Cheung, K., Ling, Z. H., Chan, C. K., and Yao, X. H.: Observation of aerosol size distribution and new particle formation at a mountain site in subtropical Hong Kong, Atmos. Chem. Phys., 12, 9923–9939, doi:10.5194/acp-12-9923-2012, 2012.

Hamed, A., Korhonen, H., Sihto, S.-L., Joutsensaari, J., Järvinen, H., Petäjä, T., Arnold, F., Nieminen, T., Kulmala, M., and Smith, J. N.: The role of relative humidity in continental new particle formation, J. Geophys. Res.-Atmos., 116, D03202, doi:10.1029/2010JD014186, 2011.

Henning, S., Weingartner, E., Schmidt, S., Wendisch, M., Gäggeler, H. W., and Baltensperger, U.: Size-dependent aerosol activation at the high-alpine site Jungfraujoch (3580 m asl), Tellus B, 54, 82–95, 2002.

Hinds, W. C.: Aerosols Technology: Properties, Behaviour and Measurement of Airborne Particles, 2nd ed., Wiley, New York, USA, 504 pp., 1999.

Hitchins, J., Morawska, L., Wolff, R., and Gilbert, D.: Concentrations of submicrometre particles from vehicle emissions near a major road, Atmos. Environ., 34, 51–59, 2000.

IPCC: Climate Change 2013: The Physical Science Basis. Contribution of Working Group I to the Fifth Assessment Report of the Intergovernmental Panel on Climate Change, edited by: Stocker, T. F., Qin, D., Plattner, G.-K., Tignor, M., Allen, S. K., Boschung, J., Nauels, A., Xia, Y., Bex, V., and Midgley, P. M., Cambridge University Press, Cambridge, United Kingdom and New York, NY, USA, 1535 pp., 2013.

Janhäll, S., Andreae, M. O., and Pöschl, U.: Biomass burning aerosol emissions from vegetation fires: particle number and mass emission factors and size distributions, Atmos. Chem. Phys., 10, 1427–1439, doi:10.5194/acp-10-1427-2010, 2010.

Kulmala, M. and Laaksonen, A.: Binary nucleation of water-sulfuric acid system: comparison of classical theories with different H_2SO_4 saturation vapor pressures, J. Chem. Phys., 93, 696–701, 1990.

ACPD
15, 25231–25267, 2015

Kulmala, M., Pirjola, L., and Mäkelä, J. M.: Stable sulphate clusters as a source of new atmospheric particles, Nature, 404, 66–69, 2000.
Kulmala, M., Maso, M., Mäkelä, J. M., Pirjola, L., Väkevä, M., Aalto, P., Miikkulainen, P., Hämeri, K., and O'Dowd, C. D.: On the formation, growth and composition of nucleation mode particles, Tellus B, 53, 479–490, 2001.
Kulmala, M., Petäjä, T., Nieminen, T., Sipilä, M., Manninen, H. E., Lehtipalo, K., Dal Maso, M., Aalto, P. P., Junninen, H., and Paasonen, P.: Measurement of the nucleation of atmospheric aerosol particles, Nat. Protoc., 7, 1651–1667, 2012.
Kusaka, I., Wang, Z. G., and Seinfeld, J. H.: Binary nucleation of sulfuric acid-water: Monte Carlo simulation, J. Chem. Phys., 108, 6829–6848, 1998.
Lehtinen, K. E. J., Korhonen, H., Maso, M. D., and Kulmala, M.: On the concept of condensation sink diameter, Boreal Environ. Res., 8, 405–412, 2003.
Lohmann, U. and Feichter, J.: Global indirect aerosol effects: a review, Atmos. Chem. Phys., 5, 715–737, doi:10.5194/acp-5-715-2005, 2005.
Mikkonen, S., Romakkaniemi, S., Smith, J. N., Korhonen, H., Petäjä, T., Plass-Duelmer, C., Boy, M., McMurry, P. H., Lehtinen, K. E. J., Joutsensaari, J., Hamed, A., Mauldin III, R. L., Birmili, W., Spindler, G., Arnold, F., Kulmala, M., and Laaksonen, A.: A statistical proxy for sulphuric acid concentration, Atmos. Chem. Phys., 11, 11319–11334, doi:10.5194/acp-11-11319-2011, 2011.
Pirjola, L., Kulmala, M., Wilck, M., Bischoff, A., Stratmann, F., and Otto, E.: Formation of sulphuric acid aerosols and cloud condensation nuclei: an expression for significant nucleation and model comprarison, J. Aerosol Sci., 30, 1079–1094, 1999.
Platt, U. and Stutz, J.: Differential Optical Absorption Spectroscopy. Principles and Applications, Springer, Berlin, Heidelberg, Germany, 2008.
Plaza, J. and Artíñano, B.: Characterization of pollutants cycles evolution in a coastal mediterranean area under summer conditions, Centro de Investigaciones Energeticas Medioambientales y Tecnologicas (CIEMAT), Madrid, Spain, 1994.
Pujadas, M., Plaza, J., Terés, J., Artíñano, B., and Millán, M.: Passive remote sensing of nitrogen dioxide as a tool for tracking air pollution in urban areas: the Madrid urban plume, a case of study, Atmos. Environ., 34, 3041–3056, 2000.
Quan, J., Tie, X., Zhang, Q., Liu, Q., Li, X., Gao, Y., and Zhao, D.: Characteristics of heavy aerosol pollution during the 2012–2013 winter in Beijing, China, Atmos. Environ., 88, 83–89, doi:10.1016/j.atmosenv.2014.01.058, 2014.

ACPD
15, 25231–25267, 2015

Robinson, A. L., Donahue, N. M., Shrivastava, M. K., Weitkamp, E. A., Sage, A. M., Grieshop, A. P., Lane, T. E., Pierce, J. R., and Pandis, S. N.: Rethinking organic aerosols: semivolatile emissions and photochemical aging, Science, 315, 1259–1262, doi:10.1126/science.1133061, 2007.

Saarikoski, S., Sillanpää, M., Sofiev, M., Timonen, H., Saarnio, K., Teinilä, K., Karppinen, A., Kukkonen, J., and Hillamo, R.: Chemical composition of aerosols during a major biomass burning episode over northern Europe in spring 2006: experimental and modelling assessments, Atmos. Environ., 41, 3577–3589, 2007.

Salvador, P.: Characterization of air pollution produced by particles in suspension in Madrid, Doctoral Thesis, Faculty of Physics, University Complutense of Madrid, Madrid, Spain, 2004.

Salvador, P., Artíñano, B., Alonso, D. G., Querol, X., and Alastuey, A.: Identification and characterisation of sources of PM_{10} in Madrid (Spain) by statistical methods, Atmos. Environ., 38, 435–447, 2004.

Salvador, P., Artíñano, B., Viana, M., Alastuey, A., and Querol, X.: Evaluation of the changes in the Madrid metropolitan area influencing air quality: analysis of 1999–2008 temporal trend of particulate matter, Atmos. Environ., 57, 175–185, 2012.

Seinfeld, J. H. and Pandis, S. N.: Atmospheric Chemistry and Physics, John Wiley and Sons, Inc., Hoboken, N.J., 1st Edn., 2006.

Shen, X. J., Sun, J. Y., Zhang, Y. M., Wehner, B., Nowak, A., Tuch, T., Zhang, X. C., Wang, T. T., Zhou, H. G., Zhang, X. L., Dong, F., Birmili, W., and Wiedensohler, A.: First long-term study of particle number size distributions and new particle formation events of regional aerosol in the North China Plain, Atmos. Chem. Phys., 11, 1565–1580, doi:10.5194/acp-11-1565-2011, 2011.

Shrivastava, M. K., Lipsky, E. M., Stanier, C. O., and Robinson, A. L.: Modeling semivolatile organic aerosol mass emissions from combustion systems, Environ. Sci. Technol., 40, 2671–2677, 2006.

Sjogren, S., Gysel, M., Weingartner, E., Alfarra, M. R., Duplissy, J., Cozic, J., Crosier, J., Coe, H., and Baltensperger, U.: Hygroscopicity of the submicrometer aerosol at the high-alpine site Jungfraujoch, 3580 m a.s.l., Switzerland, Atmos. Chem. Phys., 8, 5715–5729, doi:10.5194/acp-8-5715-2008, 2008.

Skrabalova, L., Zikova, N., and Zdimal, V.: Shrinkage of newly formed particles in an urban environment, Aerosol Air Qual. Res., 15, 1313–1324, 2015.

ACPD
15, 25231–25267, 2015

Stanier, C. O., Khlystov, A. Y., and Pandis, S. N.: Nucleation events during the Pittsburgh air quality study: description and relation to key meteorological, gas phase, and aerosol parameters special issue of aerosol science and technology on findings from the fine particulate matter supersites program, Aerosol Sci. Tech., 38, 253–264, 2004.

Vehkamäki, H., Dal Maso, M., Hussein, T., Flanagan, R., Hyvärinen, A., Lauros, J., Merikanto, P., Mönkkönen, M., Pihlatie, K., Salminen, K., Sogacheva, L., Thum, T., Ruuskanen, T. M., Keronen, P., Aalto, P. P., Hari, P., Lehtinen, K. E. J., Rannik, Ü, and Kulmala, M.: Atmospheric particle formation events at Värriö measurement station in Finnish Lapland 1998-2002, Atmos. Chem. Phys., 4, 2015–2023, doi:10.5194/acp-4-2015-2004, 2004.

Wang, S. C. and Flagan, R. C.: Scanning electrical mobility spectrometer, Aerosol Sci. Tech., 13, 230–240, 1990.

Wiedensohler, A., Birmili, W., Nowak, A., Sonntag, A., Weinhold, K., Merkel, M., Wehner, B., Tuch, T., Pfeifer, S., Fiebig, M., Fjäraa, A. M., Asmi, E., Sellegri, K., Depuy, R., Venzac, H., Villani, P., Laj, P., Aalto, P., Ogren, J. A., Swietlicki, E., Williams, P., Roldin, P., Quincey, P., Hüglin, C., Fierz-Schmidhauser, R., Gysel, M., Weingartner, E., Riccobono, F., Santos, S., Grüning, C., Faloon, K., Beddows, D., Harrison, R., Monahan, C., Jennings, S. G., O'Dowd, C. D., Marinoni, A., Horn, H.-G., Keck, L., Jiang, J., Scheckman, J., McMurry, P. H., Deng, Z., Zhao, C. S., Moerman, M., Henzing, B., de Leeuw, G., Löschau, G., and Bastian, S.: Mobility particle size spectrometers: harmonization of technical standards and data structure to facilitate high quality long-term observations of atmospheric particle number size distributions, Atmos. Meas. Tech., 5, 657–685, doi:10.5194/amt-5-657-2012, 2012.

Yao, X., Choi, M. Y., Lau, N. T., Lau, A. P. S., Chan, C. K., and Fang, M.: Growth and shrinkage of new particles in the atmosphere in Hong Kong, Aerosol Sci. Tech., 44, 639–650, 2010.

Young, L.-H., Lee, S.-H., Kanawade, V. P., Hsiao, T.-C., Lee, Y. L., Hwang, B.-F., Liou, Y.-J., Hsu, H.-T., and Tsai, P.-J.: New particle growth and shrinkage observed in subtropical environments, Atmos. Chem. Phys., 13, 547–564, doi:10.5194/acp-13-547-2013, 2013.

Zhang, R., Khalizov, A., Wang, L., Hu, M., and Xu, W.: Nucleation and growth of nanoparticles in the atmosphere, Chem. Rev., 112, 1957–2011, doi:10.1021/cr2001756, 2012.

Zhu, B., Wang, H., Shen, L., Kang, H., and Yu, X.: Aerosol spectra and new particle formation observed in various seasons in Nanjing, Adv. Atmos. Sci., 30, 1632–1644, 2013.

ACPD
15, 25231–25267, 2015

Table 1. Summary of studies related to shrinkage processes, including the present study.

Reference paper	Measurement Site	Climatic conditions	Study period	Period when the shrinkages were identified	Shrinkage Events (event type and number of cases)	Shrinkage time start (in Local Time (LT) or UTC)	Duration of the Shrinkage processes	SR* ($nm\,h^{-1}$)	Causes that lead to the shrinkage development
This study	Urban background site	Continental-Mediterranean climate	Jul 2009 to Dec 2012 (42 months)	Spring and summer seasons	NPF + shrinkage (17) Aerosol growth process + shrinkage (9) Pure shrinkage (22)	Around 18:00 UTC	From 1 to 8.5 h	Between −1 and −11.1	Atmospheric dilution and decrease in photochemical activity
Skrabalova et al. (2015)	Urban background station	Continental climate	May 2012 to Apr 2014 (24 months)	Spring and summer seasons and excepcionally autum season	NPF + shrinkage (22)	Around 12:00 UTC	> 2 h	Between −2.5 and −12.5	Atmospheric dilution, high ambient temperature and decrease in photochemical activity
Cusack et al. (2013)	Regional background station	Mediterranean climate	Oct 2010 to Jun 2011 (9 months)	Spring season	NPF + shrinkage (1) Pure shrinkage (1) Not defined in the paper (5)	Between 12:30 and 15:30 UTC	From 1 to 4 h	Between 3.1 and 11.1	High ambient temperature
Young et al. (2013)	Coastal, urban, and downwind site	Subtropical climate	Oct 2008 to Jan 2009 and Aug 2010 to Oct 2010 (7 months)	Warm season	NPF + shrinkage (5)	Between 11:09 and 13:26 LT		Between −5.1 and −7.6	Atmospheric dilution and high ambient temperature
Backman et al. (2012)	Suburban area	Subtropical climate	10 Oct 2010 to 10 Jun 2011 (9 months)	–	Pureshrinkage (1)	14:00 LT		5.2	High ambient temperature
Yao et al. (2010)	Coastal sub-urban site	Subtropical climate	Feb 2003 to Jan 2004 (12 months)	–	NPF + shrinkage (2)	12:30 and 15:00 UTC		8.6 and 10.7	Atmospheric dilution and decrease in photochemical activity

* SR can be a positive or a negative value depending on the methodology used by each author.

ACPD
15, 25231–25267, 2015

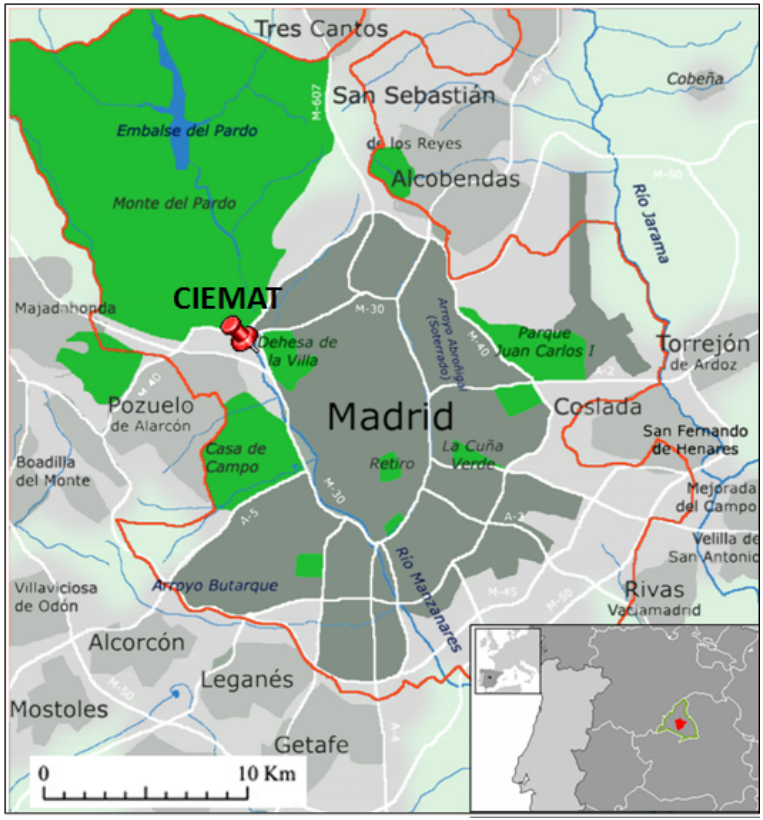

Figure 1. Location of Madrid within Spain (inset) and the measurement site at CIEMAT facilities (red marker).The red line represents the Madrid municipality and the white lines the main traffic thoroughfares.

ACPD
15, 25231–25267, 2015

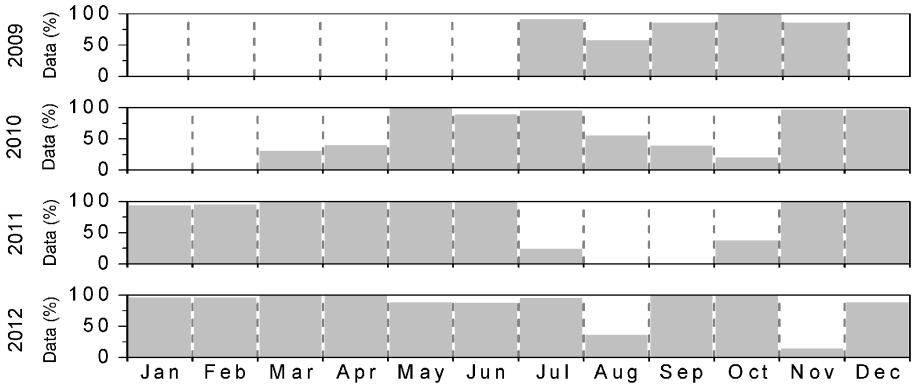

Figure 2. 2009–2012 data coverage of the submicron aerosol fraction.

ACPD
15, 25231–25267, 2015

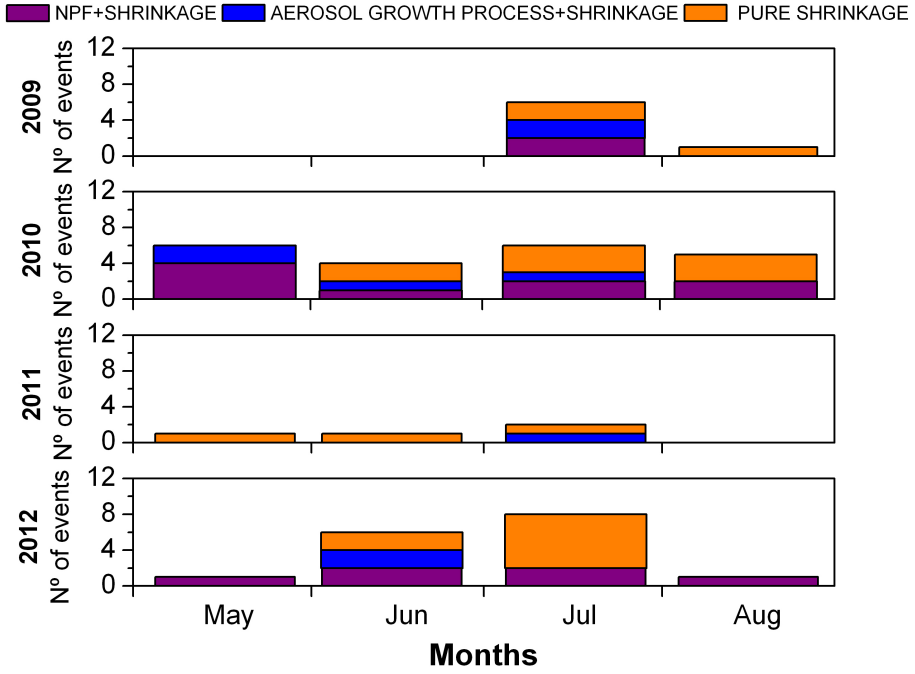

Figure 3. Interannual variation in the number and group of shrinkage events during the 3.5 years of study (data not available for May and June 2009).

ACPD
15, 25231–25267, 2015

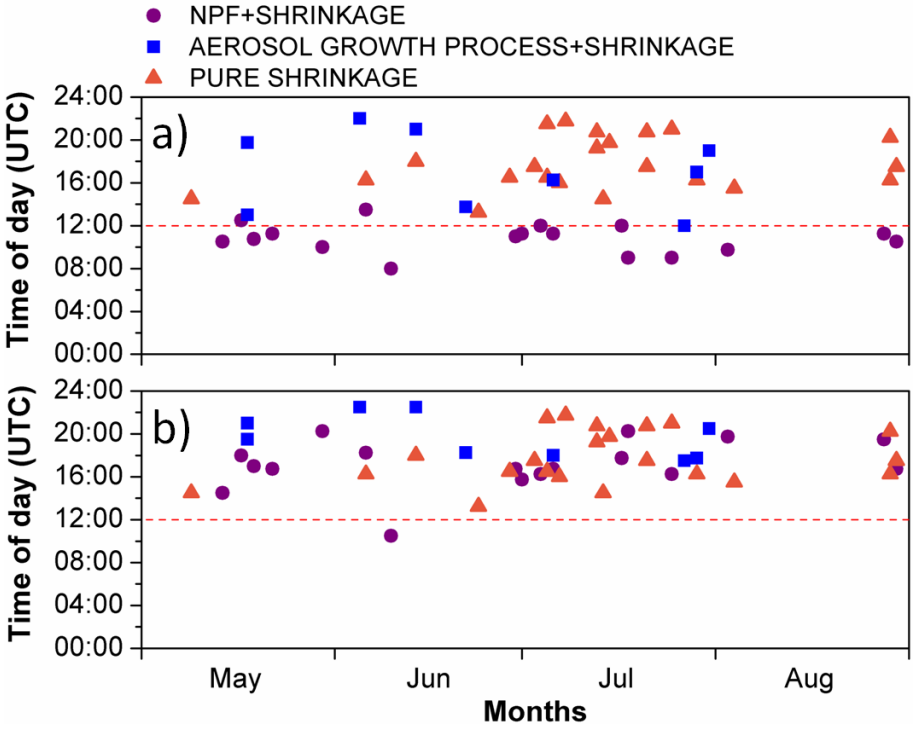

Figure 4. (a) Starting times of the shrinkage events, which includes the process that precedes the shrinkage (NPF or aerosol growth process) and the shrinkage process itself, and **(b)** starting times of the shrinkage phase (shrinkage process) during 2009–2012. The red dotted line corresponds to midday (12:00 UTC).

ACPD
15, 25231–25267, 2015

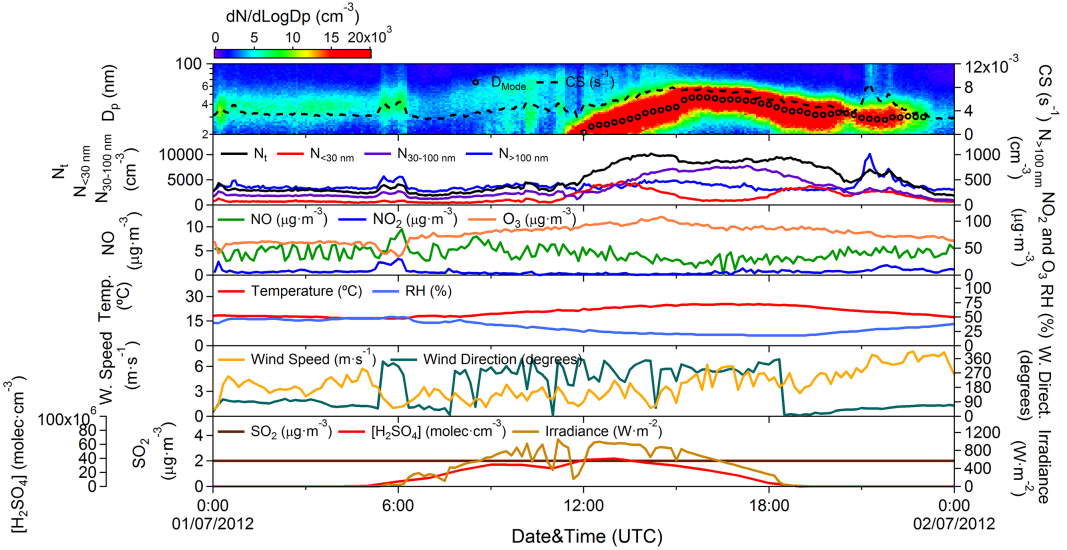

Figure 5. NPF + shrinkage case: evolution of the aerosol size distributions, total particle number concentration (N_t) and particle concentration for each of the three modes; nucleation ($N_{<30\,nm}$), Aitken ($N_{30–100\,nm}$) and accumulation ($N_{>100\,nm}$). CS, particle mode diameter (D_{mode}), NO, NO_2 and O_3 concentrations and $[H_2SO_4]$ estimation as well as meteorological conditions (temperature, relative humidity, wind speed, wind direction and irradiance) are also represented for 1 July 2012.

ACPD
15, 25231–25267, 2015

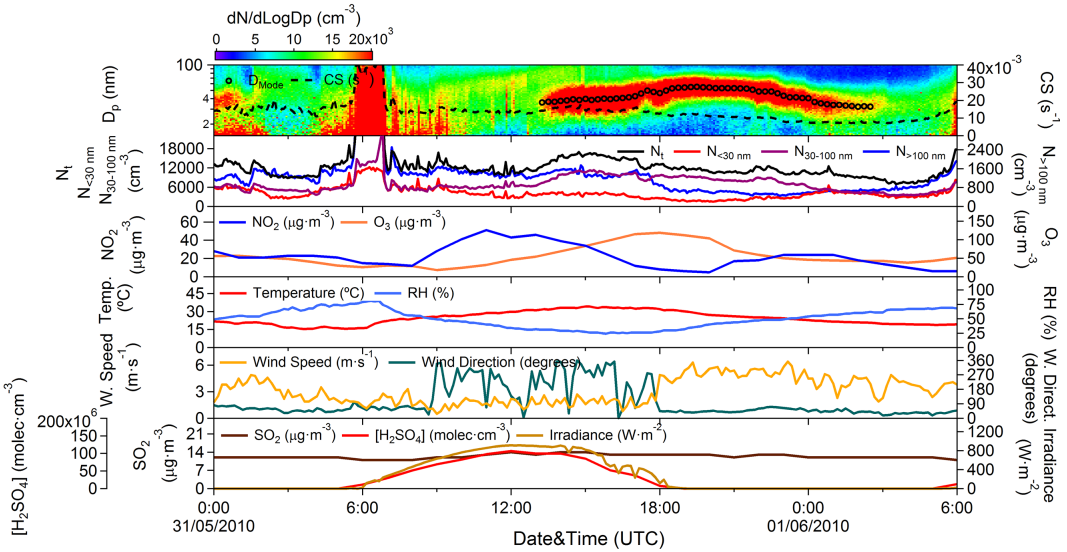

Figure 6. Aerosol growth process + shrinkage case: evolution of the aerosol size distributions, total particle number concentration (N_t) and particle concentration for each of the three modes; nucleation ($N_{<30\,nm}$), Aitken ($N_{30–100\,nm}$) and accumulation ($N_{>100\,nm}$). CS, the particle mode diameter (D_{mode}), NO_2 and O_3 concentrations and $[H_2SO_4]$ estimation as well as meteorological conditions (temperature, relative humidity, wind speed, wind direction and irradiance) are also represented for 31 May to 1 June 2010 at 06:00 UTC.

ACPD
15, 25231–25267, 2015

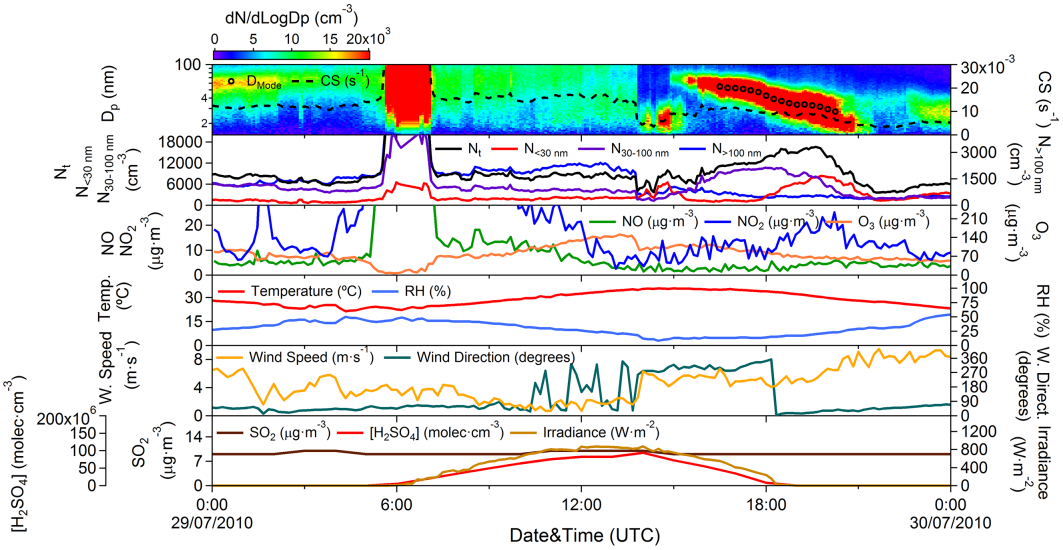

Figure 7. Pure shrinkage case: evolution of the aerosol size distributions, total particle number concentration (N_t) and particle concentration for each of the three modes; nucleation ($N_{<30\,nm}$), Aitken ($N_{30–100\,nm}$) and accumulation ($N > 100$ nm). CS, the particle mode diameter (D_{mode}), NO_2 and O_3 concentrations and $[H_2SO_4]$ estimation as well as meteorological conditions (temperature, relative humidity, wind speed, wind direction and irradiance) are also represented for 29 July 2010.

ACPD
15, 25231–25267, 2015